

Original Article

**Autophagy Attenuates MnCl₂-induced Apoptosis in Human Bronchial Epithelial Cells***

YUAN Zhun^{1,2}, YING Xian Ping³, ZHONG Wei Jian³, TIAN Shi Min⁴, WANG Yu^{1,2},
JIA Yong Rui⁵, CHEN Wen⁶, FU Juan Ling¹, ZHAO Peng^{1,2,#}, and ZHOU Zong Can^{1,#}

1. Department of Toxicology, Peking University Health Science Center, Beijing 100191, China; 2. Beijing Key Laboratory of Toxicological Research and Risk Assessment for Food Safety, Peking University Health Science Center, Beijing 100191, China; 3. Department of Toxicology, Shanghai Municipal Center for Disease Control & Prevention, Shanghai 200336, China; 4. Chinese Academy of Inspection and Quarantine Comprehensive Test Center, Beijing 100123, China; 5. Medical and Healthy Analytical Center, Peking University Health Science Center, Beijing 100191, China; 6. Department of Toxicology, Faculty of Preventive Medicine, School of Public Health, Sun Yat-sen University, Guangzhou 510080, Guangdong, China

Abstract

Objective To investigate the role of autophagy in MnCl₂-induced apoptosis in human bronchial epithelial 16HBE cells.

Methods Cell proliferation was measured by MTT assay. Mitochondrial membrane potential (MMP) and apoptosis were measured by flow cytometry. Autophagic vacuoles were detected by fluorescence microscopy. Cellular levels of apoptosis and autophagy-related proteins were measured by western blotting.

Results 16HBE cell proliferation was inhibited by MnCl₂ in a dose- and time-dependent manner. MnCl₂-induced 16HBE cell growth inhibition was related to MMP depolarization prior to the induction of apoptosis. Our data revealed that MnCl₂-induced apoptosis in 16HBE cells was mediated by decreased expression of Bcl-2 and increased levels of cleaved caspase-3. It was observed that when we exposed 16HBE cells to MnCl₂ in a dose-dependent manner, the formation of autophagic vacuoles and the levels of LC-3B-II were elevated. RNA interference of LC3B in these MnCl₂-exposed cells demonstrated that MMP loss and apoptosis were enhanced. Additionally, the pan-caspase inhibitor Z-VAD-FMK increased the cellular levels of Bcl-2 and decreased apoptosis, but did not affect the cellular levels of LC3B in MnCl₂-treated 16HBE cells.

Conclusion MnCl₂ dose- and time-dependently inhibits 16HBE cell proliferation and induces MMP loss and apoptosis. Autophagy acts in a protective role against MnCl₂-induced apoptosis in 16HBE cells.

Key words: Manganese chloride; Apoptosis; Mitochondrial membrane potential; Autophagy; 16HBE cells

Biomed Environ Sci, 2016; 29(7): 494-504

doi: 10.3967/bes2016.065

ISSN: 0895-3988

www.besjournal.com (full text)

CN: 11-2816/Q

Copyright ©2016 by China CDC

*This work was supported by National Natural Science Foundation of China (Nos. 81370079 and 81001253) and Beijing Natural Science Foundation (No. 7132122).

#Correspondence should be addressed to ZHAO Peng and ZHOU Zong Can, Tel: 86-10-82801531, E-mail: zhaopeng@bjmu.edu.cn (ZHAO Peng); zhouzcc@bjmu.edu.cn (ZHOU Zong Can).

Biographical note of the first author: YUAN Zhun, male, born in 1980, PhD, majoring in cellular and molecular toxicology.

INTRODUCTION

Manganese is a trace element and eating a small amount from food and water is needed to stay healthy^[1]. However, occupational and environmental exposure to excessive manganese is adverse to organisms. Besides causing damage to the brain, when inhaled in excess, manganese has also been implicated in inducing lung disorders^[1-3]. Apoptotic pathways are activated in the lungs of patients with acute injury, in part by activation of the membrane Fas death receptor, which results in the activation of caspase-8^[4]. Manganese chloride (MnCl₂) can dose-dependently induce apoptosis in human lung adenocarcinoma A549 cells^[5]. Manganese can also induce apoptosis in many other cells such as rat primary Leydig cells, rat astrocytes, rat astrocytoma C6 cells, and human cervical carcinoma Hela cells^[6-9]. Thus, apoptosis of alveolar epithelium might be involved in manganese-induced lung toxicity.

Autophagy is a self-digestive process in which autophagosomes combine with lysosomes and remove misfolded or aggregated proteins, clear damaged organelles, and eliminate intracellular pathogens to maintain a stable internal environment^[10]. Autophagy plays an important role in regulating cell growth, maturation, and death. Autophagy is also associated with a variety of human diseases including neurodegenerative diseases. A recent study demonstrated that MnCl₂ induces autophagy, characterized by an increase in LC3-II expression levels, the reactive oxygen species (ROS)-dependent formation of autophagic vesicles, and an increase in the Beclin1/Bcl-2 and Beclin1/Bcl-XL ratios in rat astrocytoma C6 cells. The inhibition of autophagy by 3-MA and mAtg5^{K130R} results in decreased cell viability. Moreover, *in vivo* experiments demonstrate that MnCl₂ induces injury and alters LC3 expression levels in rat striatal astrocytes^[11]. Another study demonstrates that autophagy plays a protective role against manganese-induced neuronal damage, whilst dysregulation of autophagy at later phases may mediate dopaminergic neurodegeneration in a rat model of manganism, a neurodegenerative disease associated with excessive exposure to manganese^[12]. In addition, manganese nanoparticles can effectively enter dopaminergic neuronal cells and exert neurotoxic effects by activating an apoptotic signaling pathway and autophagy^[13]. The role of

autophagy in manganese-induced neurotoxicity has been explored; however, the role of autophagy in manganese-induced lung toxicity has not yet been addressed. The human bronchial epithelial cell line 16HBE retains the morphology and characteristics of bronchial epithelial cells^[14-15], has no tumorigenicity in nude mice^[16], and can be used as an *in vitro* model of manganese-induced lung toxicity. Here, we investigated the effects of MnCl₂ on apoptosis and autophagy in 16HBE cells and determined the role of autophagy in MnCl₂-induced apoptosis.

MATERIALS AND METHODS

Chemicals and Reagents

MnCl₂ and other chemicals used in this study were purchased from Sigma-Aldrich (Sigma-Aldrich, St. Louis, MO, USA) unless specified. Reagents for cell culture were purchased from Life Technologies (Life Technologies, Gaithersburg, MD, USA). Pan-caspase inhibitor Z-VAD-FMK was purchased from Selleck Chemicals (Selleck Chemicals, Houston, TX, USA). Antibodies were purchased from Cell Signaling Technology (Cell Signaling Technology, Danvers, MA, USA). Western Blotting Luminol Reagent was purchased from TIANGEN BIOTECH (TIANGEN BIOTECH, Beijing, China). LC3B small interfering RNA (siRNA) duplexes (sc-43390) and LipofectamineTM 2000 were purchased from Santa Cruz Biotechnology (Santa Cruz Biotechnology, Santa Cruz, CA, USA) and Life Technologies, respectively.

Cell Culture

The human bronchial epithelial cell line 16HBE was a gift from Dr. DC Gruenert (University of California, San Francisco). The 16HBE cells were cultured at 37 °C and 5% CO₂ in minimum essential medium (MEM) supplemented with 10% (v/v) heat-inactivated fetal bovine serum (FBS), 10 U/mL of penicillin and 10 U/mL of streptomycin.

MTT Assay

The cells were seeded in 96-well culture plates (1×10⁴ cells per well) and 24 h later, various doses of MnCl₂ (0, 0.25, 0.5, 1, 2, or 4 mmol/L) were applied for 24 h in MEM medium containing 10% (v/v) FBS. After the treatment, the media were removed and the cells were rinsed twice with pre-warmed phosphate buffered saline (PBS). Two hundred microliters of serum-free MEM medium containing 0.4 mg/mL of MTT reagent were then added to each

well. Followed incubation with MTT for 3 h, the cells were washed twice with PBS, and then exactly 200 μL of DMSO were infused to each well. The absorbance of the solution was read at 570 nm using an ELISA reader (Bio-Rad). IC_{50} values were derived using nonlinear regression using GraphPad Prism software (GraphPad Software, Inc., La Jolla, CA, USA).

Measurement of Mitochondrial Membrane Potential (MMP) by Flow Cytometry

The cells were seeded in 25 cm^2 flasks (5×10^5 per flask) and 24 h later, various doses of MnCl_2 (0, 0.25, 0.5, 1, 2, or 4 mmol/L) were applied for 0, 1.5, 3, 6, or 24 h in MEM medium containing 10% (v/v) FBS. After the treatment, the cells were harvested by centrifugation at 800 g for 5 min, washed twice with PBS, and stained with 10 $\mu\text{g/mL}$ of rhodamine 123 at 37 $^\circ\text{C}$ in the dark for 30 min. After incubation with the fluorescent probes, the cells were washed twice with PBS, and the fluorescent signals were measured using a flow cytometer (BD FACSCalibur, Franklin Lakes, NJ, USA).

Measurement of Apoptosis by Flow Cytometry

The measurement of apoptosis by flow cytometry was carried out as described previously^[17]. The cells were seeded in 25 cm^2 flasks (5×10^5 cells per flask) and 24 h later, various doses of MnCl_2 (0, 0.25, 0.5, 1, 2, or 4 mmol/L) were applied for 0, 1.5, 3, 6, or 24 h in MEM medium containing 10% (v/v) FBS. After incubation with MnCl_2 , the cells were harvested by centrifugation at 800 g for 5 min, washed twice with PBS, and labeled with Annexin V-FITC, together with propidium iodide (PI) according to the manufacturer's instructions (BD Biosciences). Fluorescent signals were measured using a flow cytometer (BD FACSCalibur, Franklin Lakes, NJ, USA). The results are presented as the percentages of cells that were in early apoptosis (Annexin V⁺ PI⁻), late apoptosis (Annexin V⁺ PI⁺), or necrosis (Annexin V⁻ PI⁺).

Detection of Autophagic Vacuoles by Monodansyl Cadaverine (MDC) Staining Assay

The formation of autophagic vacuoles induced by MnCl_2 treatment was detected by MDC staining assay. The cells were plated in 24-well culture plates with glass coverslips (2×10^4 cells per well) and 24 h later, various doses of MnCl_2 (0, 0.25, 0.5, 1, 2, or 4 mmol/L) were applied for 24 h in MEM medium

containing 10% (v/v) FBS. After the treatment, the cells were washed twice with PBS, and stained with 50 $\mu\text{mol/L}$ of MDC in PBS at 37 $^\circ\text{C}$ in the dark for 45 min. After incubation with MDC, the cells were washed four times with PBS, then analyzed by fluorescence microscopy (Nikon E400).

Western Blotting

The total cellular proteins were extracted as described previously^[18]. Protein concentration was determined using the Bradford protein assay. Cell extracts containing 30 μg of proteins were separated on 14% (w/v) SDS-PAGE gels and transferred to a nitrocellulose membrane (Pall). After 2 h blocking with 5% (w/v) nonfat milk in TBST (1.5 mol/L of NaCl, 20 mmol/L of Tris-HCl, 0.05% (v/v) Tween-20, pH 7.4), the nitrocellulose membrane was incubated overnight at 4 $^\circ\text{C}$ with Bax, Bcl-2, caspase-3, Beclin-1, Atg5, LC3B, or actin antibodies (at 1:1000 dilutions). The blots were then washed four times with TBST prior 1.5 h incubation at room temperature with horseradish peroxidase-conjugated secondary antibody (at 1:10,000 dilutions). The protein bands were detected by Western Blotting Luminol Reagent and recorded on Kodak films. The images were acquired using a Canon LiDE220 scanner and analyzed by Quantity One software (Bio-Rad).

RNA Interference (RNAi) Experiment

The 16HBE cells were cultured in 6-well plates and transfected at 50% confluence. The siRNA transfection was performed using LipofectamineTM 2000, essentially following the manufacturer's procedure, with 10 μL /well of lipid reagent and 100 pmol /well of siRNA oligomer in a 6-well plate. Six hours after transfection, 2% (v/v) FBS was added and the cells were cultured for another 30 h before MnCl_2 treatment. The siRNA efficiency was verified by western blotting.

Statistical Analysis

Data were expressed as the mean \pm standard deviation. All statistical analysis was performed in SPSS for windows (SPSS, Inc., Chicago, IL). Experimental comparisons between treatments were made by one-way ANOVA followed by Dunnett's post hoc test or two-way ANOVA followed by Bonferroni's post hoc test. $P < 0.05$ was considered to indicate statistical significance. All experiments were performed in triplicate.

RESULTS

Effects of MnCl₂ on Cell Proliferation in 16HBE Cells

The cells were treated with MnCl₂ (0, 0.25, 0.5, 1, 2, or 4 mmol/L) for 24 h and MTT assay was conducted to determine the inhibitory effect of MnCl₂ on cell proliferation. As shown in Figure 1A, MnCl₂ inhibited 16HBE cell proliferation in a dose-dependent manner. The IC₅₀ values of MnCl₂ treatment at 24 h were 1.88±0.24 mmol/L.

Dose-dependent Decrease in MMP and Increase in Apoptosis Induced by MnCl₂ in 16HBE Cells

Mitochondria play important roles in programmed cell death, especially apoptosis. To investigate the effects of MnCl₂ on the functional state of mitochondria, 16HBE cells were treated with MnCl₂ (0, 0.25, 0.5, 1, 2, or 4 mmol/L) for 24 h, then the MMP levels were determined by flow cytometry. The results are shown in Figure 1B. Compared with untreated cells, the mean fluorescence intensities of MMP dose-dependently decreased in 1, 2, and 4 mmol/L MnCl₂-treated cells. These results indicate that mitochondrial dysfunction was induced by MnCl₂ treatment in 16HBE cells.

MnCl₂-induced apoptosis was then determined by flow cytometry. The results are shown in Figure 2A. The flow cytometry scatters are shown in supplementary Figure S1. During the observation period, only 2 and 4 mmol/L MnCl₂ induced significant levels of apoptosis. These results indicated that the inhibitory effects of 2 and

4 mmol/L MnCl₂ on cell proliferation in 16HBE cells were partly due to MnCl₂-induced apoptosis.

To explore the possible molecular mechanisms underlying MnCl₂-induced apoptosis, the cellular levels of apoptosis-related proteins Bax, Bcl-2, and caspase-3 (including full-length procaspase-3 and cleaved caspase-3) were determined by western blotting. The results are shown in Figure 2B-2E. The decrease in Bcl-2 levels and the Bcl-2/Bax ratio and the increase in cleaved caspase-3 levels were induced by MnCl₂ in a dose-dependent manner. In addition, compared with untreated cells, the cellular levels of Bax decreased in 4 mmol/L MnCl₂-treated cells, and the cellular levels of full length procaspase-3 increased in 1 and 2 mmol/L MnCl₂-treated cells and decreased in 4 mmol/L MnCl₂-treated cells.

Time-dependent Decrease in MMP and Increase in Apoptosis Induced by MnCl₂ in 16HBE Cells

The decrease in MMP and Bcl-2 levels were concurrent with apoptosis in 2 mmol/L MnCl₂-treated 16HBE cells at 24 h. To clarify whether these effects induced by MnCl₂ treatment are the signals leading to cell death or the secondary effects of cell death, the effects of MnCl₂ (2 mmol/L) on MMP and apoptosis at earlier time points (0, 1.5, 3, and 6 h) were determined. The results are shown in Figure 3. MnCl₂ (2 mmol/L) time-dependently induced a decrease in MMP (Figure 3A), an increase in apoptosis (Figure 3B), and a decrease in Bcl-2 levels (Figure 3C and 3D) and the Bcl-2/Bax ratio (Figure 3E). MnCl₂-induced apoptosis was observed at 6 h. The

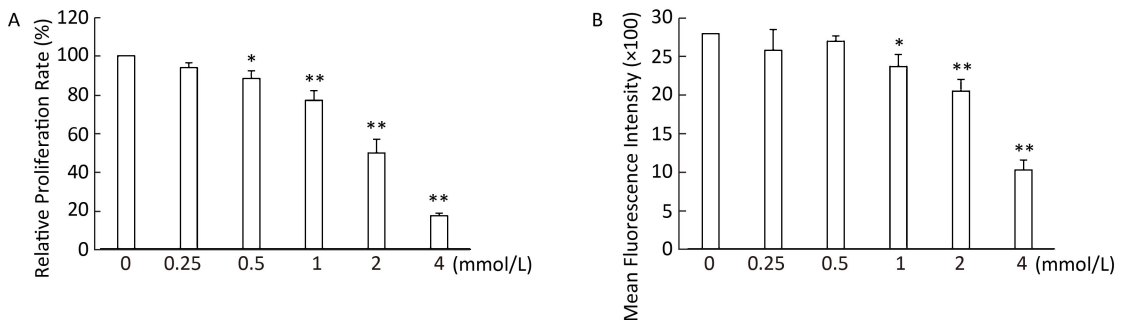


Figure 1. Dose-dependent effects of MnCl₂ on cell proliferation and MMP in 16HBE cells. The cells were treated with MnCl₂ (0, 0.25, 0.5, 1, 2, or 4 mmol/L) for 24 h. After the treatment, cell proliferation and MMP were determined by MMT assay and flow cytometry, respectively. (A) The results of relative proliferation rates. Each value represents a mean±standard error of three experiments. (B) Mean fluorescence intensities of MMP. Each value represents a mean±standard deviation of three experiments. **P*<0.05, ***P*<0.01, compared with the untreated control (0 mmol/L) group.

significant changes in MMP and Bcl-2 induced by 2 mmol/L MnCl₂ were first observed at 1.5 and 3 h, respectively, earlier than MnCl₂-induced apoptosis. These results indicated that the decrease of MMP and Bcl-2 levels might be the signals leading to apoptosis not the secondary effects of cell death.

MnCl₂-induced Autophagy in 16HBE Cells

The 16HBE cells were treated with MnCl₂ (0, 0.25, 0.5, 1, 2, or 4 mmol/L) for 24 h. The formation of

autophagic vacuoles was detected by the MDC staining assay. The expression levels of autophagy-related proteins Beclin-1, Atg5, and LC3B (including LC3B-I and LC3B-II) were determined by western blotting. The results are shown in Figure 4. The formation of autophagic vacuoles (Figure 4C-4H), the cellular levels of LC3B-II (Figure 4I and 4J), and the ratio of LC3B-II to LC3B-I (Figure 4K) dose-dependently increased in 0.5, 1, and 2 mmol/L MnCl₂-treated cells, and decreased in 4 mmol/L MnCl₂-treated cells. The cellular levels of Beclin-1, Atg5,

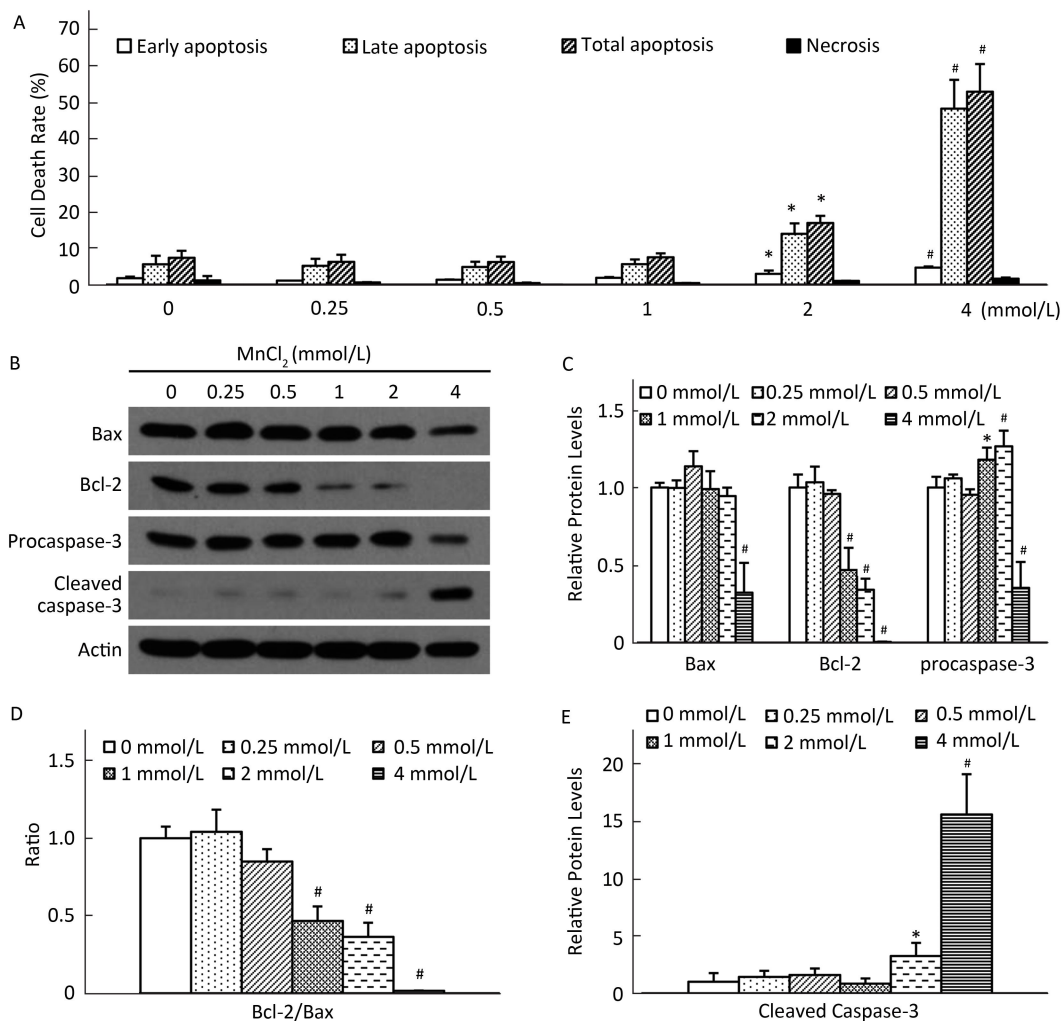


Figure 2. Dose-dependent effects of MnCl₂ on apoptosis and apoptosis-related proteins (Bax, Bcl-2, and caspase-3) levels in 16HBE cells. The cells were treated with MnCl₂ (0, 0.25, 0.5, 1, 2, or 4 mmol/L) for 24 h. After the treatment, the cells were labeled with Annexin V-FITC/PI, and then analyzed by flow cytometry. The cellular levels of Bax, Bcl-2, and caspase-3 (including full length procaspase-3 and cleaved caspase-3) were determined by western blotting. (A) Results of MnCl₂-induced apoptosis. The results are presented as the percentages of cells that were in early apoptosis (Annexin V⁺ PI⁻), late apoptosis (Annexin V⁺ PI⁺) or necrosis (Annexin V⁻ PI⁺). (B) Representative immunoblot obtained with Bax, Bcl-2, caspase-3, and actin antibodies. (C-E) Densitometric analysis of (B). The value of the untreated control (0 mmol/L) group was set to 1. Each value represents a mean±standard deviation of three experiments. **P*<0.05, #*P*<0.01 compared with the untreated control (0 mmol/L) group.

and LC3B-I (Figure 4I and 4J) decreased in 4 mmol/L MnCl₂-treated cells. These results indicated that autophagy was induced by MnCl₂ (0.5-2 mmol/L) in 16HBE cells.

Effects of LC3B Downregulation by RNAi on MnCl₂-induced MMP Loss and Apoptosis in 16HBE Cells

To determine the roles of autophagy in MnCl₂-induced mitochondrial dysfunction and apoptosis, 16HBE cells were transfected with LC3B siRNA and 36 h later, treated with 0, 1, or 2 mmol/L of MnCl₂ for 24 h. The MMP and apoptosis were measured by flow cytometry. The results are shown in Figures 5 and 6. Compared with the MOCK (transfection reagent group) cells, the cellular levels of LC3B-I and LC3B-II significantly decreased in LC3B

siRNA-transfected cells treated with 0, 1, and 2 mmol/L MnCl₂ at 24 h (Figure 5). The LC3B-II downregulation by RNAi was concurrent with the significant decrease in MMP in 1 and 2 mmol/L MnCl₂-treated cells (Figure 6A) as well as the significant increase in apoptosis (Figure 6B) in 0, 1, and 2 mmol/L MnCl₂-treated cells. Notably, compared with the untransfected cells, the cellular levels of LC3B-I and LC3B-II significantly increased in MOCK cells treated with 0, 1, and 2 mmol/L MnCl₂ at 24 h (Figure 5). These results indicate that the transfection procedure enhanced autophagy in 16HBE cells. Moreover, the enhancement of autophagy by the transfection procedure counteracted apoptosis induced by 2 mmol/L MnCl₂ in 16HBE cells (Figure 6B).

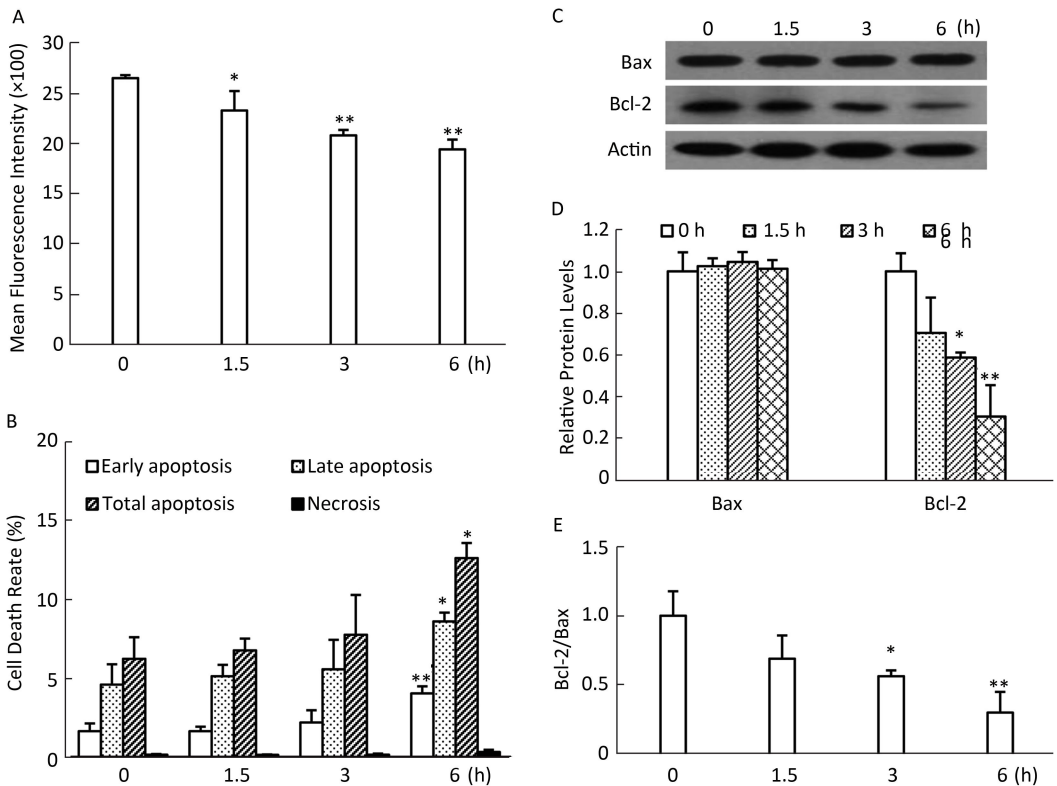


Figure 3. Time-dependent effects of MnCl₂ on MMP, apoptosis, and apoptosis-related protein (Bax and Bcl-2) levels in 16HBE cells. The cells were treated with 2 mmol/L MnCl₂ for 0, 1.5, 3, or 6 h. After the treatment, the cells were labeled with rhodamine 123 or Annexin V-FITC/PI, respectively, and then analyzed by flow cytometry. The cellular levels of Bax and Bcl-2 were determined by western blotting. (A) Mean fluorescence intensities of MMP. (B) Results of MnCl₂-induced apoptosis. The results are presented as the percentages of cells that were in early apoptosis (Annexin V⁺ PI⁻), late apoptosis (Annexin V⁺ PI⁺), or necrosis (Annexin V⁻ PI⁺). (C) Representative immunoblot obtained with Bax, Bcl-2, and actin antibodies. (D) and (E) Densitometric analysis of (C). The value of 0 h was set to 1. Each value represents a mean±standard deviation of three experiments. **P*<0.05, ***P*<0.01, compared with 0 h.

Effects of Pan-caspase Inhibitor Z-VAD-FMK on Apoptosis and Cellular Levels of Bax, Bcl-2, and LC3B in 2 mmol/L MnCl₂-treated 16HBE Cells

To determine the effects of apoptosis inhibition on MnCl₂-induced autophagy in 16HBE cells, the cells were treated with 50 μmol/L pan-caspase inhibitor Z-VAD-FMK and 30 min later, 2 mmol/L MnCl₂ was applied for 24 h. After the treatment, apoptosis and the cellular levels of Bax, Bcl-2, and LC3B in 16HBE cells

were determined by flow cytometry and western blotting, respectively. The results are shown in Figure 7. Z-VAD-FMK significantly decreased apoptosis (Figure 7A) and increased Bcl-2 levels and the Bcl-2/Bax ratio in 2 mmol/L of MnCl₂-treated 16HBE cells (Figure 7B-E). In addition, Z-VAD-FMK significantly increased the cellular levels of LC3B-II in untreated (0 mmol/L) 16HBE cells, but did not affect the cellular levels of LC3B-I and LC3B-II in 2 mmol/L MnCl₂-treated 16HBE cells (Figure 7B, 7F, and 7G).

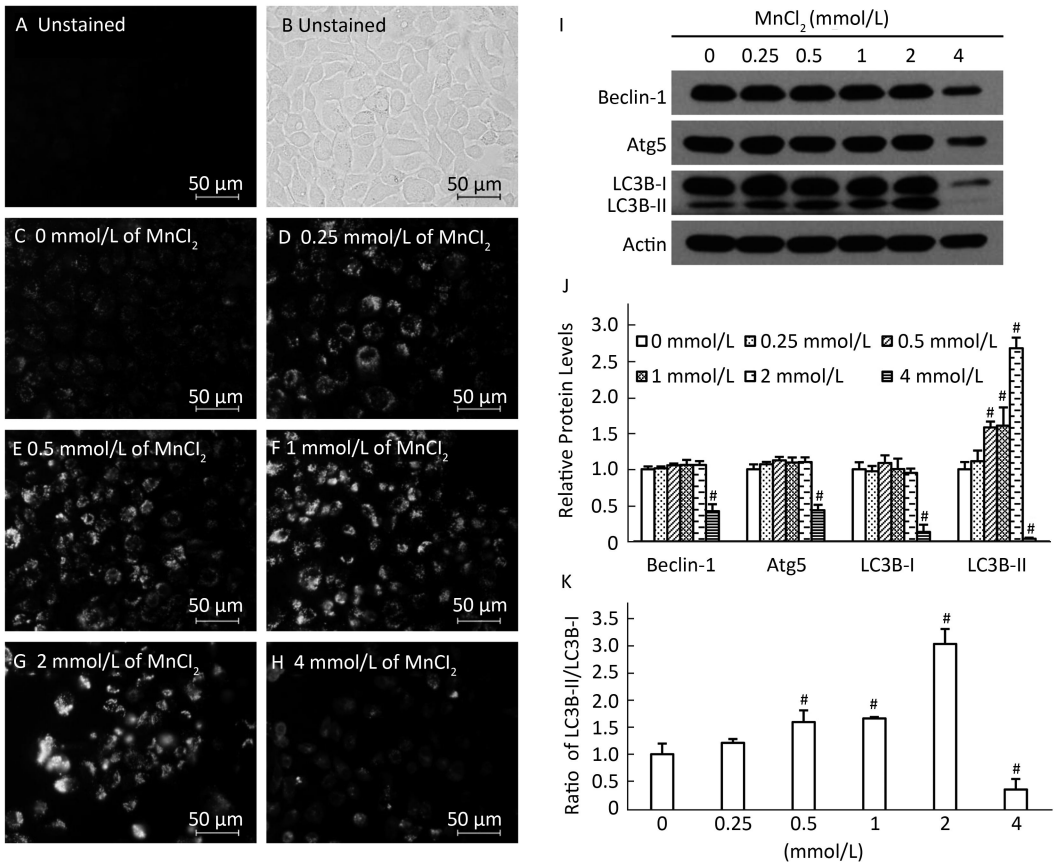


Figure 4. MnCl₂-induced autophagy in 16HBE cells. The cells were treated with MnCl₂ (0, 0.25, 0.5, 1, 2, or 4 mmol/L) for 24 h. After the treatment, the formation of autophagic vacuoles was detected by MDC staining assay, and the cellular levels of autophagy-related proteins Beclin-1, Atg5, and LC3B were determined by western blotting. (A-H) Results of MDC staining assay. (I) Representative immunoblot obtained with Beclin-1, Atg5, LC3B, and actin antibodies. (J) Densitometric analysis of (I). (K) Ratio of LC3B-II to LC3B-I. The value of untreated control (0 mmol/L) group was set to 1. Each value represents a mean±standard deviation of three experiments. #*P*<0.01 compared with the untreated control (0 mmol/L) group.

DISCUSSION

Up to now, the molecular mechanisms underlying manganese-induced lung toxicity have not been well understood. Our previous study found that MnCl₂ can induce apoptosis in human lung adenocarcinoma A549 cells in a dose-dependent manner^[5]. Here, we further investigated the effects of MnCl₂ on cell proliferation, mitochondrial function,

and apoptosis in 16HBE cells, as well as the role of autophagy in MnCl₂-induced apoptosis. We found that MnCl₂ induced cell proliferation inhibition, MMP loss, and apoptosis in 16HBE cells in a dose- and time-dependent manner. Autophagy prevented 16HBE cells from undergoing apoptosis when the cells were exposed to MnCl₂.

The available evidence indicates that manganese exposure can result in both cellular injury and impaired repair, two key events that contribute to the manifestation of toxicity. Epithelial injury, including apoptotic cell death, is an important

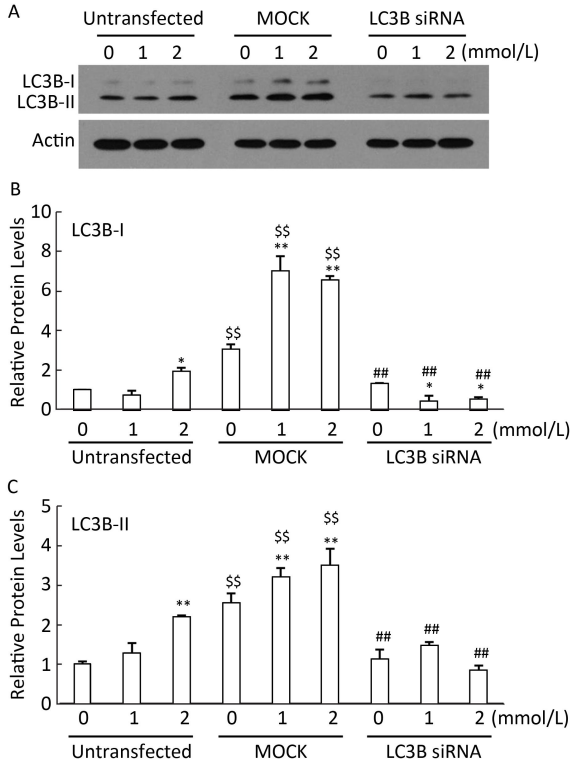


Figure 5. Effects of LC3B siRNA transfection on the cellular levels of LC3B in 16HBE cells. The cells were transfected with LC3B siRNA and 36 h later, treated with 0, 1, or 2 mmol/L MnCl₂ for 24 h. After the treatment, the cellular levels of LC3B were determined by western blotting. (A) Representative immunoblot obtained with LC3B and actin antibodies. (B) and (C) Densitometric analysis of (A). The value of the untreated control (0 mmol/L) in the untransfected group was set to 1; each value represents a mean±standard deviation of three experiments. **P*<0.05, ***P*<0.01 compared with the untreated control (0 mmol/L) group. ##*P*<0.01 compared with MOCK. \$\$*P*<0.01 compared with the untransfected group.

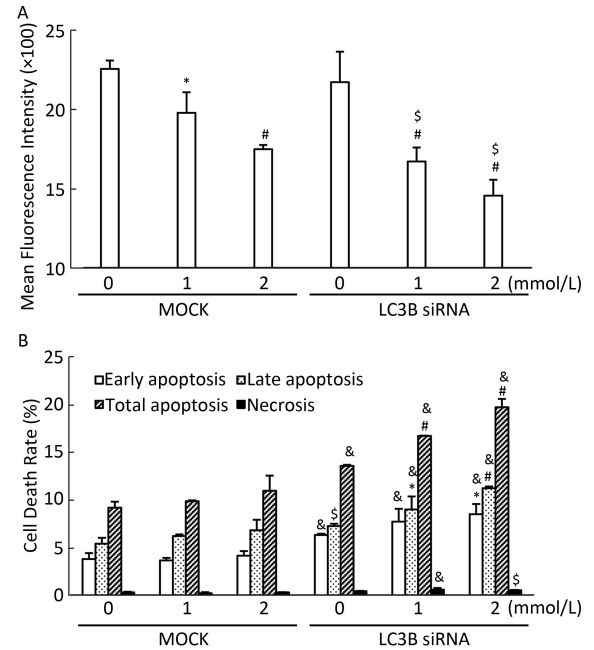


Figure 6. Effects of suppression of LC3B by RNAi on MnCl₂-induced MMP loss and apoptosis in 16HBE cells. The cells were transfected with LC3B siRNA and 36 h later, treated with 0, 1, or 2 mmol/L MnCl₂ for 24 h. After the treatment, the cells were labeled with rhodamine 123 or Annexin V-FITC/PI, respectively, then analyzed by flow cytometry. (A) Mean fluorescence intensities of MMP. (B) Results of MnCl₂-induced apoptosis. The results are presented as the percentages of cells that were in early apoptosis (Annexin V⁺ PI⁻), late apoptosis (Annexin V⁺ PI⁺), or necrosis (Annexin V⁻ PI⁺). Each value represents a mean±standard deviation of three experiments. **P*<0.05, #*P*<0.01 compared with the untreated control (0 mmol/L) group. \$*P*<0.05, &*P*<0.01 compared with MOCK.

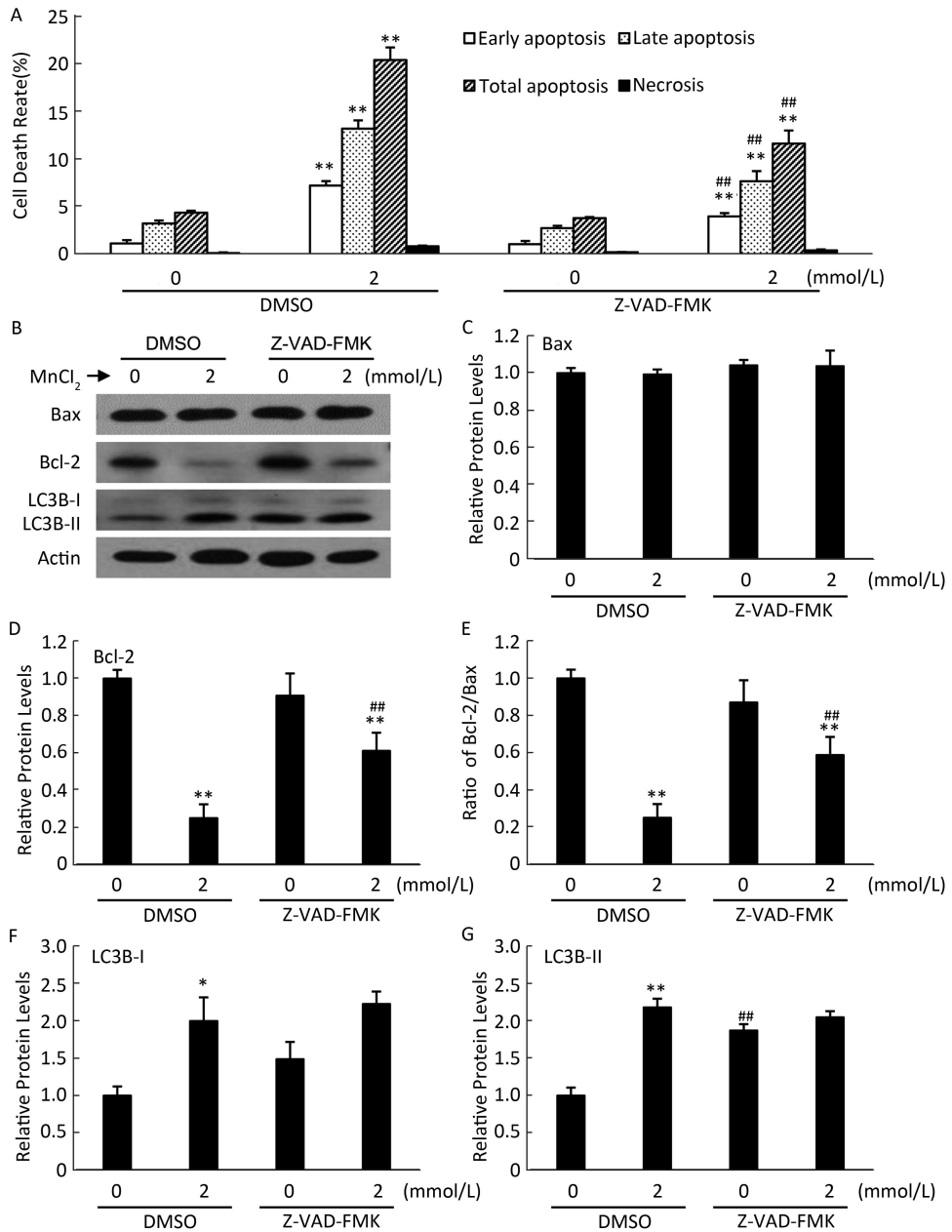


Figure 7. Effects of Z-VAD-FMK on apoptosis and the cellular levels of Bax, Bcl-2, and LC3B in MnCl₂-treated 16HBE cells. The cells were treated with 50 μ mol/L of Z-VAD-FMK and 30 min later, 2 mmol/L MnCl₂ was applied for 24 h. After the treatment, the cells were labeled with Annexin V-FITC/PI, then analyzed by flow cytometry. The cellular levels of Bax, Bcl-2, and LC3B were determined by western blotting. (A) Results of MnCl₂-induced apoptosis. The results are presented as the percentages of cells that were in early apoptosis (Annexin V⁺ PI⁻), late apoptosis (Annexin V⁺ PI⁺), or necrosis (Annexin V⁻ PI⁺). (B) Representative immunoblot obtained with Bax, Bcl-2, LC3B, and actin antibodies. (C-G) Densitometric analysis of (B). The value of the untreated control (0 mmol/L) in the DMSO group was set to 1. Each value represents a mean \pm standard deviation of three experiments. * P <0.05, ** P <0.01 compared with the untreated control (0 mmol/L) group. ### P <0.01 compared with the DMSO group.

characteristic in the pathogenesis of lung disease. Manganese induces apoptosis in rat cortical astrocytes and rat astrocytoma C6 cells by initiating the mitochondrial apoptotic pathway^[7-8]. The current study demonstrated that MnCl₂ dose- and time-dependently induced MMP loss and apoptosis in human bronchial epithelial 16HBE cells. MnCl₂-induced MMP loss was earlier than MnCl₂-induced apoptosis. In addition, MnCl₂-induced apoptosis was concurrent with the increase in cleaved caspase-3 and the decrease in Bcl-2 and full-length procaspase-3. All of these results indicate that MnCl₂ induces apoptosis by evoking mitochondrial apoptotic programs. Besides inducing apoptosis, manganese also disrupts the cell cycle. Our previous study has demonstrated that MnCl₂ treatment can induce human lung carcinoma A549 cell G0/G1 and S phase arrest within a sublethal dose^[5]. Manganese-induced cell cycle arrest has also been found in many other cells such as primary human astrocytes, primary rat Leydig cells and PC12 cells^[6,19-20]. Cell proliferation is an important part of the process of tissue repair. Manganese might arrest cell cycle progression, the basis of cell proliferation, and thereby impair the repair process.

Autophagy is a unique mechanism of clearing damaged organelles and protein aggregates in mammalian cells. Besides maintaining cell homeostasis and ensuring cell survival under stressful conditions, autophagy participates in the regulation of cell death, especially apoptotic pathways. In this study, MnCl₂-induced autophagy was observed in 16HBE cells. The doses (0.5, 1, and 2 mmol/L) needed to induce autophagy are lower than those (2 and 4 mmol/L) needed to induce apoptosis. Downregulation of LC3B by RNAi increased MMP loss and apoptosis in 1 and 2 mmol/L MnCl₂-treated 16HBE cells. Moreover, the enhancement of autophagy by the transfection procedure counteracted apoptosis induced by 2 mmol/L MnCl₂ in 16HBE cells. These results indicate that autophagy might be an adaptive stress response prior to apoptotic cell death and may act as a protector to promote cell survival when the cells are exposed to MnCl₂. Notably, it has been reported that LipofectamineTM 2000-mediated transport of negative control siRNAs dose- and time-dependently induced an increase in autophagosomes in Huh7.5 and H4IIE hepatoma cells^[21]. Thus, LipofectamineTM 2000 might be the main cause of the increase of LC3B in MOCK cells (Figure 5). Mitophagy, the selective autophagy of damaged mitochondria, is

considered to be the central mechanism of mitochondrial quality and quantity control^[22]. The degradation of damaged mitochondria can impede apoptotic pathways by preventing mitochondrial outer membrane permeabilization and the subsequent release of proapoptotic molecules such as cytochrome c^[23-24]. MnCl₂-induced mitophagy has been demonstrated by an increase in LC3 and TOM-20 colocalization in rat astrocytoma C6 cells^[11]. Autophagy inhibition by downregulating LC3B might impair the elimination of damaged mitochondria, and thereby evoke apoptotic programs and enhance MnCl₂-induced apoptosis. The mechanisms by which autophagy counteracts apoptosis need further investigation.

It should be noted that this study focuses on exploring the role of autophagy in MnCl₂-induced 16HBE cell apoptosis. Thus, the doses (1 and 2 mmol/L) that at which MnCl₂ induces those effects are relatively high and in most cases, not relevant to the environment or workplace. The manganese concentration in the blood of healthy adults is reported to range from 4 to 15 µg/L, with an average value of approximately 9 µg/L^[1]. Workers in industries using or producing manganese are the most likely to have higher exposures to manganese, primarily due to inhalation of manganese dust in workplace air, as compared to the general population. It has been reported that the average airborne manganese levels (total dust) in the breathing zone of two factories located in China were 0.24 and 2.21 mg/m³. The greatest levels were observed during welding operations in enclosed spaces, and were much higher than the Occupational Safety and Health Administration time-weighted average Permissible Exposure Limit of 1 mg total manganese/m³^[1]. However, due to the lack of sufficient relevant toxicokinetic data on the one hand, and on the other hand, the multitude of factors such as exposure duration, respiratory rate and depth that might affect the target concentrations of human bronchial epithelial cell exposure to manganese by inhalation, it is difficult to achieve an extrapolation between the target concentrations in the bronchial epithelium and the concentrations in the exposure air.

In summary, MnCl₂ dose- and time-dependently inhibits 16HBE cell proliferation and induces MMP loss and apoptosis. Autophagy acts in a protective role against MnCl₂-induced apoptosis in 16HBE cells.

Received: April 19, 2016;

Accepted: June 28, 2016

REFERENCES

1. Agency for Toxic Substances and Disease Registry. Toxicological profile for manganese. 2012.
2. Barceloux DG. Manganese. *J Toxicol Clin Toxicol*, 1999; 37, 293-307.
3. Corradi M, Mutti A. Metal ions affecting the pulmonary and cardiovascular systems. *Met Ions Life Sci*, 2011; 8, 81-105.
4. Martin TR, Hagimoto N, Nakamura M, et al. Apoptosis and epithelial injury in the lungs. *Proc Am Thorac Soc*, 2005; 2, 214-20.
5. Zhao P, Zhong W, Ying X, et al. Manganese chloride-induced G0/G1 and S phase arrest in A549 cells. *Toxicology*, 2008; 250, 39-46.
6. Cheng J, Fu J, Zhou Z. The mechanism of manganese-induced inhibition of steroidogenesis in rat primary Leydig cells. *Toxicology*, 2005; 211, 1-11.
7. Gonzalez LE, Juknat AA, Venosa AJ, et al. Manganese activates the mitochondrial apoptotic pathway in rat astrocytes by modulating the expression of proteins of the Bcl-2 family. *Neurochem Int*, 2008; 53, 408-15.
8. Alaimo A, Gorojod RM, Kotler ML. The extrinsic and intrinsic apoptotic pathways are involved in manganese toxicity in rat astrocytoma C6 cells. *Neurochem Int*, 2011; 59, 297-308.
9. Oubrahim H, Stadtman ER, Chock PB. Mitochondria play no roles in Mn(II)-induced apoptosis in HeLa cells. *Proc Natl Acad Sci U S A*, 2001; 98, 9505-10.
10. Noda NN, Inagaki F. Mechanisms of Autophagy. *Annu Rev Biophys*, 2015; 44, 101-22.
11. Gorojod RM, Alaimo A, Porte Alcon S, et al. The autophagolysosomal pathway determines the fate of glial cells under manganese-induced oxidative stress conditions. *Free Radic Biol Med*, 2015; 87, 237-51.
12. Zhang J, Cao R, Cai T, et al. The role of autophagy dysregulation in manganese-induced dopaminergic neurodegeneration. *Neurotox Res*, 2013; 24, 478-90.
13. Afeseh Ngwa H, Kanthasamy A, Gu Y, et al. Manganese nanoparticle activates mitochondrial dependent apoptotic signaling and autophagy in dopaminergic neuronal cells. *Toxicol Appl Pharmacol*, 2011; 256, 227-40.
14. Cozens AL, Yezzi MJ, Kunzelmann K, et al. CFTR expression and chloride secretion in polarized immortal human bronchial epithelial cells. *Am J Respir Cell Mol Biol*, 1994; 10, 38-47.
15. Pang Y, Li W, Ma R, et al. Development of human cell models for assessing the carcinogenic potential of chemicals. *Toxicol Appl Pharmacol*, 2008; 232, 478-86.
16. Zhao P, Fu J, Yao B, et al. In vitro malignant transformation of human bronchial epithelial cells induced by benzo(a)pyrene. *Toxicol In Vitro*, 2012; 26, 362-8.
17. Zhao P, Fu J, Yao B, et al. Diethyl sulfate-induced cell cycle arrest and apoptosis in human bronchial epithelial 16HBE cells. *Chem Biol Interact*, 2013; 205, 81-9.
18. Zhao P, Zhong W, Ying X, et al. Comparative proteomic analysis of anti-benzo(a)pyrene-7,8-dihydrodiol-9,10-epoxide-transformed and normal human bronchial epithelial G0/G1 cells. *Chem Biol Interact*, 2010; 186, 166-73.
19. Sengupta A, Mense SM, Lan C, et al. Gene expression profiling of human primary astrocytes exposed to manganese chloride indicates selective effects on several functions of the cells. *Neurotoxicology*, 2007; 28, 478-89.
20. Zhao F, Zhang JB, Cai TJ, et al. Manganese induces p21 expression in PC12 cells at the transcriptional level. *Neuroscience*, 2012; 215, 184-95.
21. Mo RH, Zaro JL, Ou JH, et al. Effects of Lipofectamine 2000/siRNA complexes on autophagy in hepatoma cells. *Mol Biotechnol*, 2012; 51, 1-8.
22. Wei H, Liu L, Chen Q. Selective removal of mitochondria via mitophagy: distinct pathways for different mitochondrial stresses. *Biochim Biophys Acta*, 2015; 1853, 2784-90.
23. Kim I, Rodriguez-Enriquez S, Lemasters JJ. Selective degradation of mitochondria by mitophagy. *Arch Biochem Biophys*, 2007; 462, 245-53.
24. Wang Y, Nartiss Y, Steipe B, et al. ROS-induced mitochondrial depolarization initiates PARK2/PARKIN-dependent mitochondrial degradation by autophagy. *Autophagy*, 2012; 8, 1462-76.